

Supplementary Materials for

Ultrafast chemical imaging by widefield photothermal sensing of infrared absorption

Yeran Bai, Delong Zhang, Lu Lan, Yimin Huang, Kerry Maize, Ali Shakouri*, Ji-Xin Cheng*

*Corresponding author. Email: jxcheng@bu.edu (J.-X.C.); shakouri@purdue.edu (A.S.)

Published 19 July 2019, *Sci. Adv.* **5**, eaav7127 (2019)

DOI: 10.1126/sciadv.aav7127

The PDF file includes:

Section S1. Simulation and experimental results for film samples

Section S2. Estimation of maximum probe power saturating the camera sensor

Fig. S1. Simulation and experimental results for film samples.

Fig. S2. Widefield photothermal imaging of living cells at different depths.

Other Supplementary Material for this manuscript includes the following:

(available at advances.sciencemag.org/cgi/content/full/5/7/eaav7127/DC1)

Movie S1 (.avi format). Movie clip showing the time-resolved imaging of the transient thermal process of a 486-nm-thick polymer film.

Movie S2 (.avi format). Movie clip showing an ultrafast imaging speed of 1250 frames/s of a 486-nm-thick polymer film.

Section S1. Simulation and experimental results for film samples

The photothermal image contrast is created by detecting the difference of reflected photon intensity at hot and cold states (**fig. S1a**). The structure resembles the multi-layer thin-film coatings with the native oxide layer on silicon neglected. We used the parameters of Poly(methyl methacrylate) (PMMA) for simulations (34): $dn/dT = -1.41 \times 10^{-4} \text{K}^{-1}$ and $dL/dT = 2.48 \times 10^{-4} \text{K}^{-1}$. The reflection at cold state R was plotted with blue solid curve in **fig. S1b**, where strong oscillation was due to interference effect. For the hot state, we updated the refractive index and thickness in Eq. 1 with the estimated temperature increase of 8 K and plotted the reflection R' with red dashed curve in **fig. S1b**. The zoom-in view of the R and R' curves revealed the extremely small difference that we need to extract for signal. The normalized reflection difference calculated by $(R' - R)/R$ was plotted in **fig. S1c** with the solid black curve. To validate the modelling, we performed the experiments with four PMMA thickness of 249 nm, 278 nm, 333 nm and 486 nm. The maximum signal for each thickness was normalized and plotted in **fig. S1c** with red dots. A good agreement was observed between simulation and experimental results.

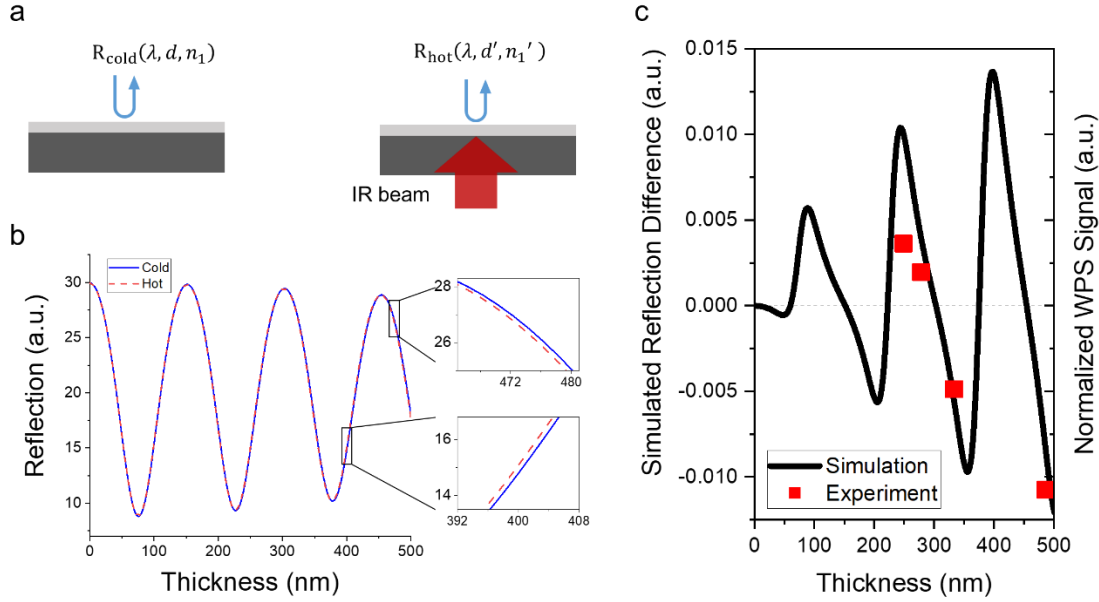


Fig. S1. Simulation and experimental results for film samples. (a) Schematic of photothermal detection of light reflection. The signal is generated by detecting the reflection difference as a function of probe beam wavelength, refractive index, and sample thickness. (b) Simulated reflection curve at cold (blue solid) and hot (red dashed) states for the sample thickness ranging from 0 to 500 nm. PMMA was used as the sample. The temperature increase was set to be 8 K. Expanded views show the reflection difference between hot and cold states. (c) Simulated reflection difference versus sample thickness (black curve) and the measured photothermal signal at four example thicknesses (red squares).

Section S2. Estimation of maximum probe power saturating the camera sensor

The visible probe power density to saturate the camera sensor (Lince 5M, AnaFocus) can be calculated as

$$I = \frac{S_0}{A \times \text{QE}} = 1310 \text{ photons}/\mu\text{m}^2 \quad (\text{S.1})$$

where S_0 is the full well capacity: 19000 e^- , A is the pixel area: $25 \mu\text{m}^2$ and the quantum efficiency (QE) of 58% at 450 nm. For $\lambda = 450 \text{ nm}$, energy per photon is $4.4\text{e}^{-19} \text{ J}$, corresponding

to 1.1×10^{-15} W for 400 μ s camera integration time. Therefore, the saturation probe power reaching the sensor is

$$1310 \text{ (photons}/\mu\text{m}^2) \times 1.1 \times 10^{-15} \text{ (W)} \times 25 \text{ (}\mu\text{m}^2) \times 2560 \times 2048 \text{ (pixels)} = 0.19 \text{ mW}$$

Consider the 50/50 beam splitter loss and sample surface reflection ratio $\sim 27\%$, $\sim 14\%$ of incident power at sample reaches the sensor. Therefore, the maximum power incident on the sample is around 1.4 mW. Deviations from probe spot size and the collection efficiency of the objective are not considered here. Overall, the probe power on the mW level is expected for the given camera sensor and integration time.

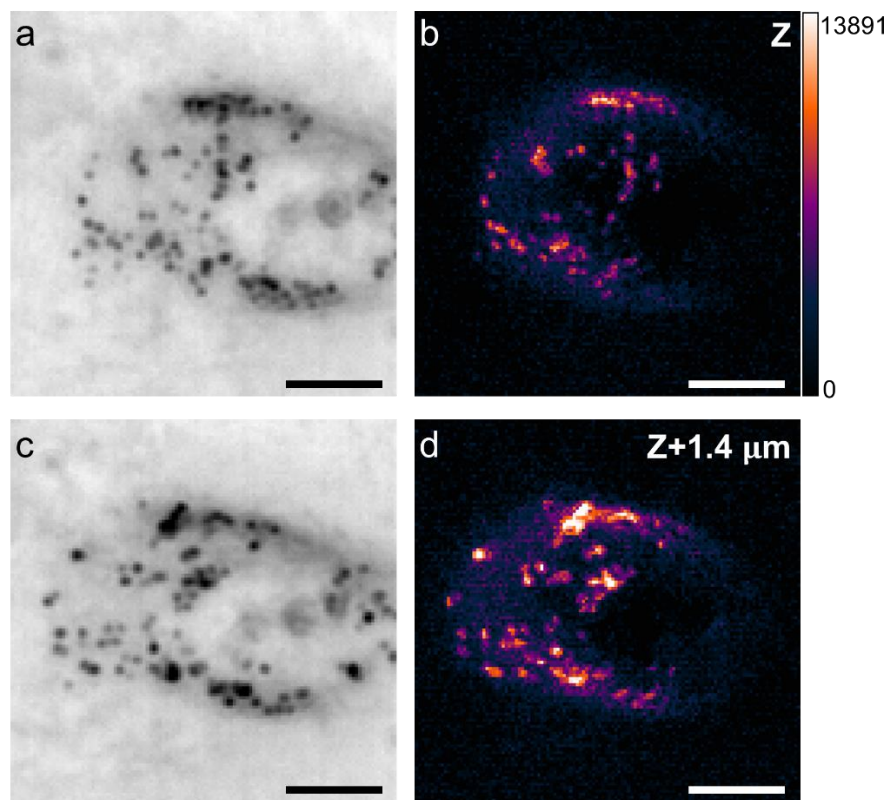


Fig. S2. Widefield photothermal imaging of living cells at different depths. (a-b) Reflection image and photothermal image with IR tuned to 1744 cm^{-1} targeting C=O bond in lipid droplets. (c-d) Corresponding images at different depth position. Imaging speed, 2 Hz. Scale bars, 10 μ m.